

Supporting information

Förster Resonance Energy Transfer-Based Dual-Modal Theranostic Nanoprobe for In Situ Visualization of Cancer Photothermal Therapy

Dehong Hu¹, Zonghai Sheng^{1*}, Mingting Zhu¹, Xiaobing Wang¹, Fei Yan¹, Chengbo Liu², Liang Song², Ming Qian¹, Xin Liu¹, and Hairong Zheng^{1*}

¹ Paul C. Lauterbur Research Center for Biomedical Imaging, Institute of Biomedical and Health Engineering, Shenzhen Institutes of Advanced Technology, Chinese Academy of Sciences, Shenzhen 518055, P. R. China.

² Research Laboratory for Biomedical Optics and Molecular Imaging, Shenzhen Key Laboratory for Molecular Imaging, Institute of Biomedical and Health Engineering, Shenzhen Institutes of Advanced Technology, Chinese Academy of Sciences, Shenzhen 518055, China.

*Corresponding author: Hairong Zheng and Zonghai Sheng

E-mail: hr.zheng@siat.ac.cn; zh.sheng@siat.ac.cn.

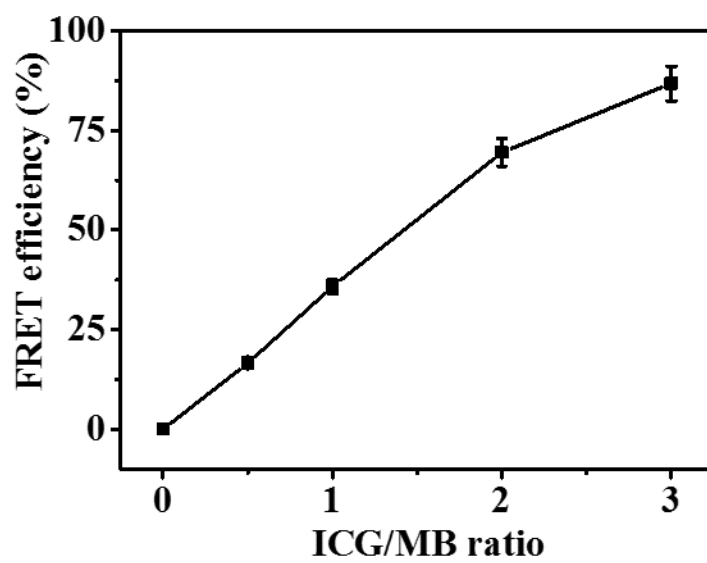


Figure S1. The FRET efficacy of HSA-ICG-MB complex with different ICG/MB ratios.

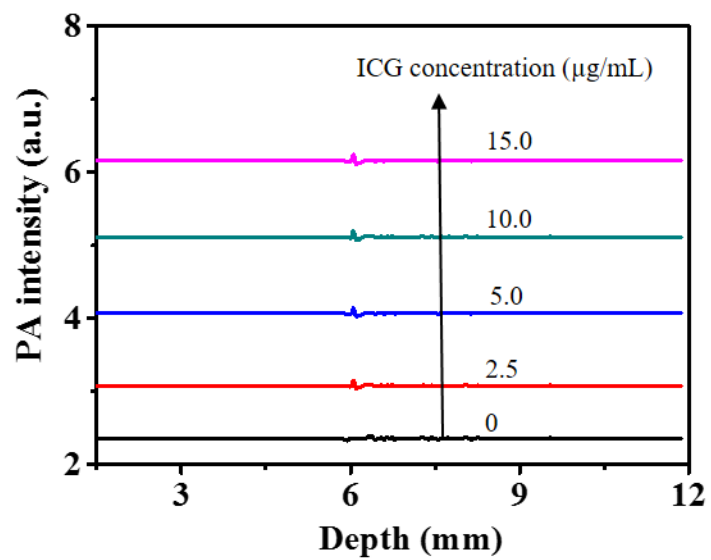


Figure S2. PA signal of ICG at different concentrations.

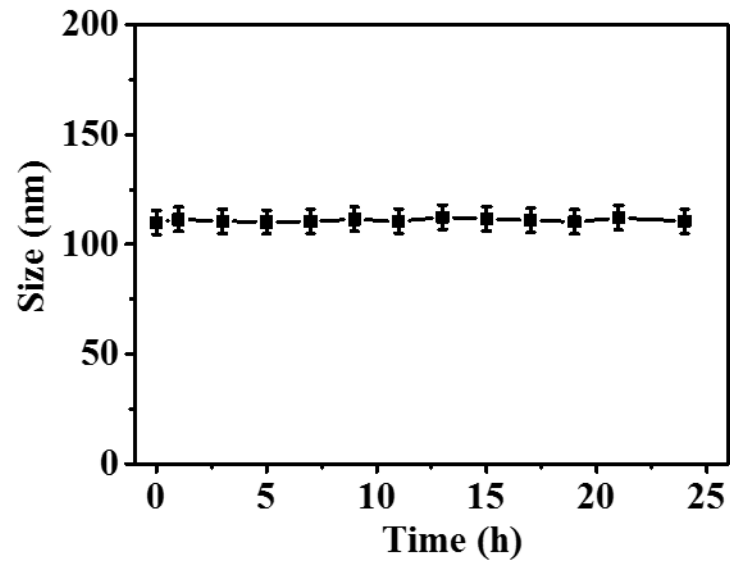


Figure S3. The size changes of HSA-ICG-MB NPs in PBS at 37 °C.

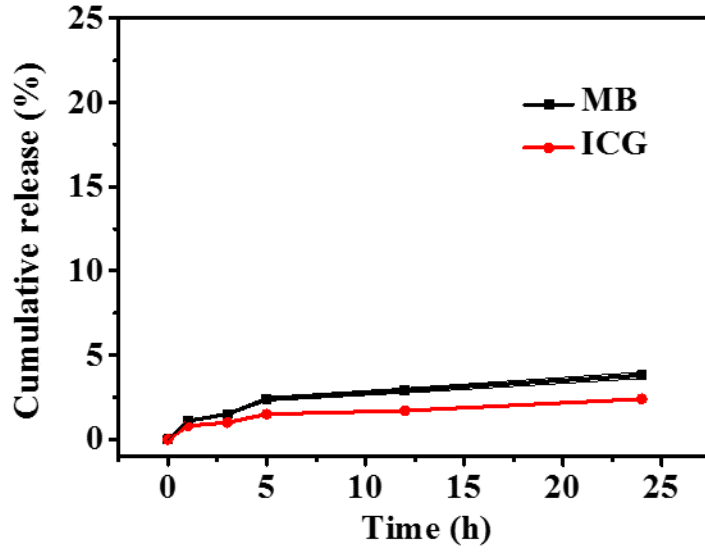


Figure S4. *In vitro* release profile of HSA-ICG-MB NPs in PBS (pH=7.4).

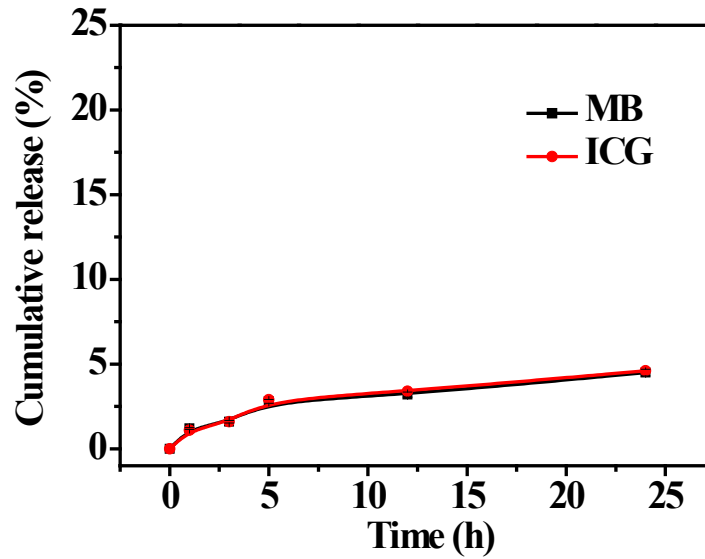


Figure S5. *In vitro* release profile of HSA-ICG-MB NPs in serum.

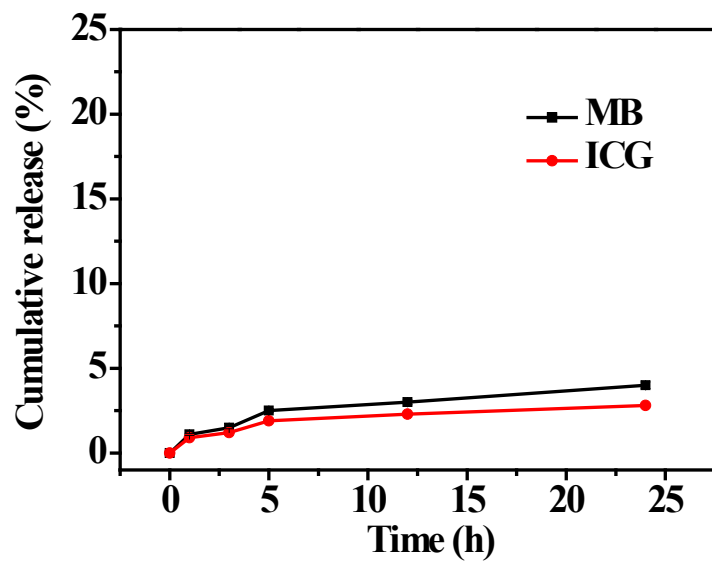


Figure S6. *In vitro* release profile of HSA-ICG-MB NPs in medium.

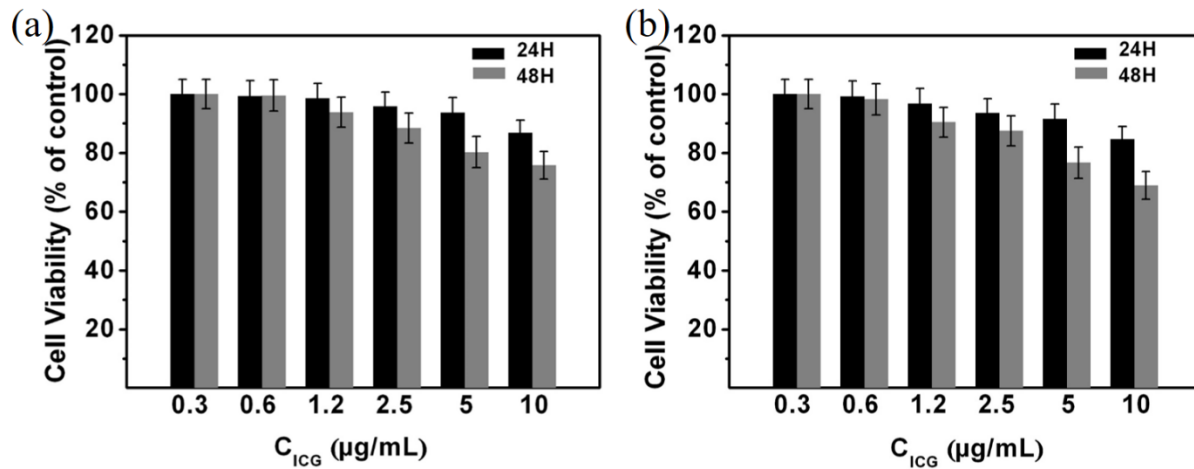


Figure S7. Cell viabilities of bEnd.3 endothelial cells (a) and C6 glioma cells (b) incubated with NPs at different concentrations for 24 h and 48 h.

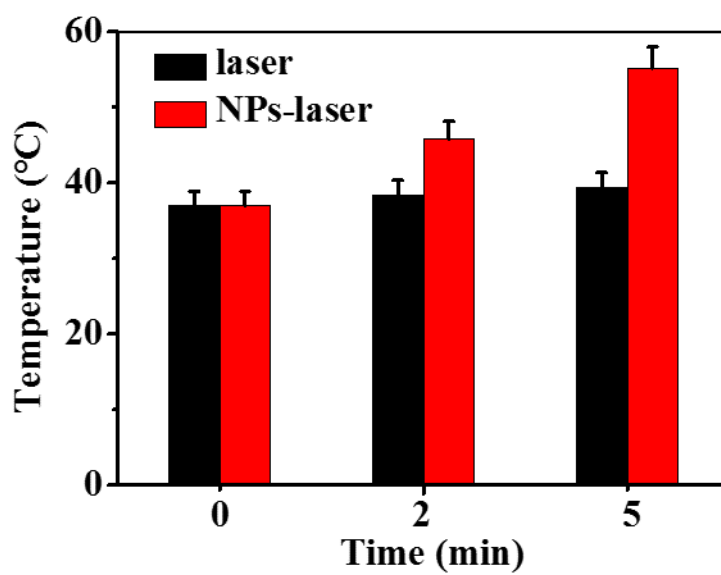


Figure S8. Time-dependent temperature generation of C6 glioma cells upon NIR laser irradiation (808 nm, 1.0 W/cm²).

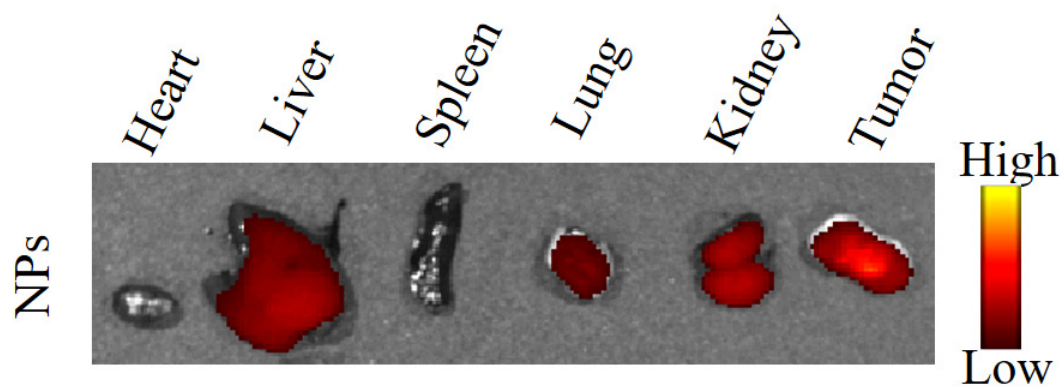


Figure S9. Ex vivo fluorescence images of major organs and tumors after injection of HSA-ICG-MB NPs at 24 h.

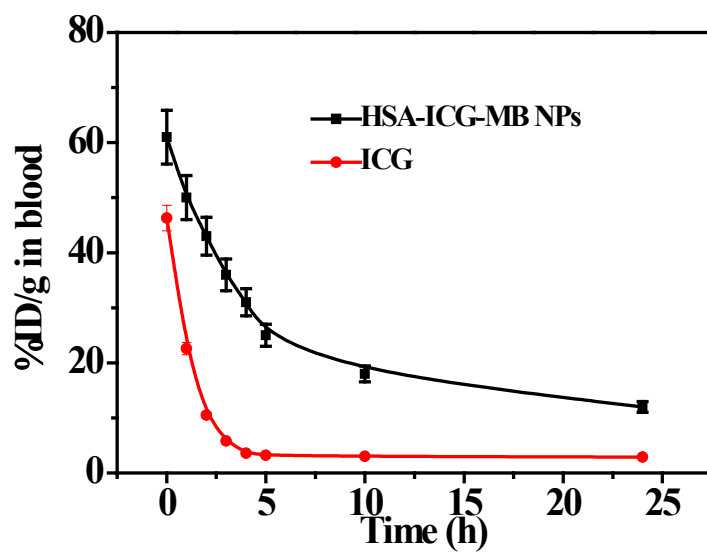


Figure S10. Pharmacokinetics curve of HSA-ICG-MB NPs and ICG determined based on ICG fluorescence in the blood lysates.

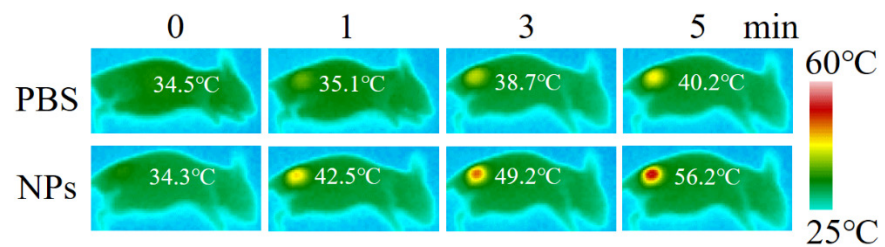


Figure S11. Infrared thermal images of C6 tumor-bearing mice exposed to 808-nm laser for 5 min (0.8 W/cm^2).

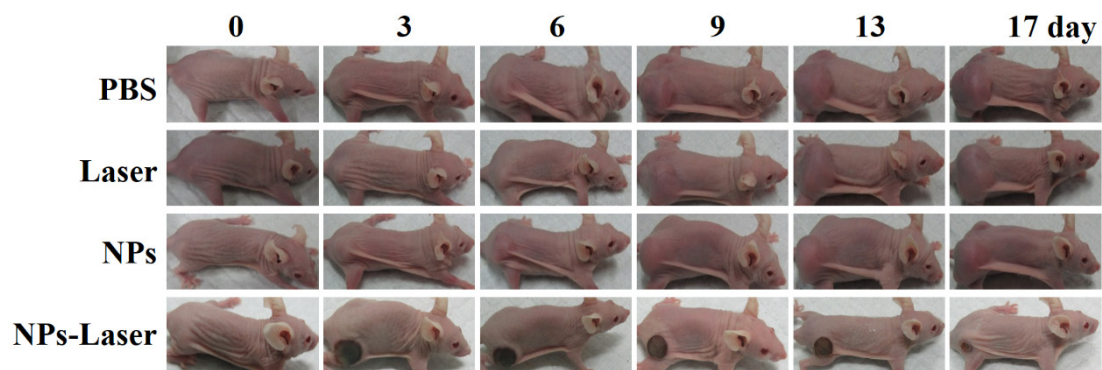


Figure S12. Photographs of mice with different treated groups.

Table S1 Loading efficiency (LE), Size distribution, Zeta potential, and FRET efficacy of HAS-ICG-MB NPs. The data were shown as mean \pm SD (n = 3).

	LE-MB	LE-ICG	Size (nm)	Zeta Potential (mv)	FRET efficacy (%)
1	0%	8.6%	100 \pm 3.2	-34.5 \pm 0.8	----
2	2.2%	7.3%	110 \pm 2.9	-33.8 \pm 0.4	88.2
3	4.8%	3.9%	115 \pm 4.6	-34.8 \pm 0.5	32.4
4	6.8%	2.6%	125 \pm 3.7	-34.5 \pm 0.4	13.2
5	8.7%	0%	121 \pm 3.9	-34.8 \pm 0.5	0.0